

Improvement DTC for Induction Motor Drives Using Modern Speed Controllers Tuning by PSO Algorithm

Brahim Kiyyour^{1*}, Louanasse Laggoun², Ahmed Salhi^{1,3}, Djemai Naimi^{1,3}, Ghoulemallah Boukhalifa⁴

¹ Department of Electrical Engineering, Faculty of Sciences and Technology, University of Biskra, 07000 Biskra, P.O.B. 145 RP, Algeria

² Department of Industrial Engineering, Faculty of Sciences and Technology, University of Khenchela, 40004 Khenchela, P.O.B. 1252, Algeria

³ Laboratory of Electrical Engineering (LGEB), University of Biskra, 07000 Biskra, P.O.B. 145 RP, Algeria

⁴ Department of Electrical Engineering, Faculty of Sciences and technology, University of Batna, 05078 Batna, P.O.B. 53, Algeria

* Corresponding author, e-mail: brahim.kiyyour@univ-biskra.dz

Received: 13 August 2022, Accepted: 06 February 2023, Published online: 06 April 2023

Abstract

The work carried out in this paper proposes an improvement of the direct torque control (DTC) of induction machine by the design of modern, robust and more efficient controllers than the conventional PI controllers commonly used for speed control. A comparative study has been carried out using five controllers, i.e. PI anti-windup, first-order sliding mode control (SMC), second order sliding mode control (SOSMC), fuzzy logic controller (Fuzzy-PI) and hybrid Fuzzy second-order sliding mode controller (FSOSMC). An advanced optimization technique based on the particle swarm optimization (PSO) algorithm has been utilized to optimize all of these controllers, the use of PSO for the determination of the different gains used in all controllers gives on the one hand a high accuracy performance and ensures on the other hand a reliable comparison between the different controllers in their optimal states. The simulation and analysis of each method with respect to robustness to disturbances was performed externally under various operating conditions and variations of the machine parameters.

Keywords

direct torque control, induction machine, first sliding mode control, second sliding mode control, fuzzy logic, particle swarm optimization

1 Introduction

The DTC, or direct torque control, is the most efficient control technique for induction motors. It has many advantages [1, 2]. However, it offers above all exceptional dynamic performance in open loop to say without resorting to a speed or position sensor on the motor shaft, so it seems to be particularly advantageous for most standard industrial applications, however, for complex and very sensitive applications, essentially those with speed precision requirements, it will be catered by using a sensor and thus implementing a closed loop control. The performance of the closed loop control translates into excellent dynamic performance, particularly in terms of reaction speed of the drive when applying a torque step corresponding to the nominal value, a dynamic speed precision; this depends on the controller used and the gain setting of that controller. On the other side, the use of PI controller for speed control has many disadvantages: indeed, these controllers

are linear and cannot control nonlinear systems with variable parameters [3, 4].

Moreover, when the controlled part is subject to strong non-linearity and temporal variations, it is necessary to design control algorithms that ensure the robustness of the control strategy against the variations of the model uncertainty parameters [5].

Recently, artificial intelligence and nonlinear techniques such as fuzzy logic and controllers based on high-order sliding mode theory have received increasing attention in solving complex and practical problems; they are widely applied in the electrical machine domain [6–8].

By solving the problem of sensitivity to internal parametric variations of the machine and external perturbations, this work aims at enhancing the robustness and stability of the DTC control algorithm by replacing conventional linear PI controllers with modern controllers,

including PI anti-Windup, first-order and second-order sliding mode based on super-twisting algorithm (SMC and SOSMC), Fuzzy-PI and hybrid Fuzzy second-order sliding mode controllers (FSOSMC) [9, 10].

The determination of the different gains in the different controllers used is often a difficult and complex process that requires a lot of calculations, moreover these calculations often lack accuracy, and sometimes researchers are forced to use the trial and error method to determine or modify them [11, 12], so to avoid such problems we have used in this paper the PSO technique in order to achieve two important goals, the first is to ensure an optimal setting of the gains of the speed controllers, while the second one is to put all the controllers in a situation of equal and fair comparison.

The efficiency of different control techniques will be examined by simulation using Matlab/Simulink software.

In this paper, a detailed analysis and comparative simulation study between DTC-PI Anti-Windup, DTC-SMC, DTC-SOSMC, DTC-Fuzzy and DTC-FSOSMC is performed.

The study is carried out mainly for electric vehicle (EV) applications, unmanned aerial vehicles, robotics and all applications requiring accurate and fast speed response, especially in areas exposed to severe climatic conditions such as extreme heat or cold. With this study, manufacturers have a wide range of options to choose a controller that is suitable for their industrial needs.

Finally, to prove the feasibility and performance of these approaches, simulations and a comparison are presented to demonstrate the contribution of these approaches.

2 Modeling of induction machine

In the synchronous (d - q) reference frame rotating at ω_s speed, the model of induction motor is given by Eq. (1) and Eq. (2):

$$\begin{aligned} v_{ds} &= R_s i_{ds} + \frac{d\varphi_{ds}}{dt} - \omega_s \varphi_{qs} \\ v_{qs} &= R_s i_{qs} + \frac{d\varphi_{qs}}{dt} + \omega_s \varphi_{ds} \\ 0 &= R_r i_{dr} + \frac{d\varphi_{dr}}{dt} - (\omega_s - \omega_r) \varphi_{qr} \\ 0 &= R_r i_{qr} + \frac{d\varphi_{qr}}{dt} + (\omega_s - \omega_r) \varphi_{dr} \end{aligned} \quad (1)$$

Stator and Rotor flux components:

$$\begin{aligned} \varphi_{ds} &= L_s i_{ds} + L_m (i_{ds} + i_{dr}) \\ \varphi_{qs} &= L_s i_{qs} + L_m (i_{qs} + i_{qr}) \\ \varphi_{dr} &= L_r i_{dr} + L_m (i_{ds} + i_{dr}) , \\ \varphi_{qr} &= L_r i_{qr} + L_m (i_{qs} + i_{qr}) \\ L_m &= \frac{3}{2} L_{sr} = \frac{3}{2} L_{rs} \end{aligned} \quad (2)$$

where L_m is the cyclic mutual inductance between stator and rotor.

The electromagnetic torque of the motor can be expressed by Eq. (3):

$$T_e = p(\varphi_{ds} i_{qs} - \varphi_{qs} i_{ds}), \quad (3)$$

and mechanical equation by Eq. (4):

$$J \frac{d\Omega}{dt} = T_e - T_r - f_r \Omega. \quad (4)$$

3 Direct torque control of induction motor

Direct torque control is a research strategy for the speed control of the induction motor fed by a variable frequency converter. It controls the torque on the basis of maintaining the invariant flux value by choosing the voltage space vector [13–15].

In its basic principle, direct torque control is a method based on switching tables with torque and stator flux hysteresis. With this method, the number of inverter switching operations is minimised, the stator torque/flux are decoupled, the inverter is controlled without a PWM generator, the open-loop parameters are estimated in the stator reference frame and the control is provided without mechanical sensors. The basic DTC scheme is shown in Fig. 1.

The expressions of the stator voltages allow us to calculate, in real time and at any time, the flux and torque magnitudes, using Eqs. (5) and (6).

$$\begin{aligned} \varphi_{s\alpha} &= \int_0^t (V_{s\alpha} - R_s i_{s\alpha}) \\ \varphi_{s\beta} &= \int_0^t (V_{s\beta} - R_s i_{s\beta}) \end{aligned} \quad (5)$$

Hence, the stator flux module is written (Eq. (6)):

$$\varphi_s = \sqrt{(\varphi_{s\alpha})^2 + (\varphi_{s\beta})^2}. \quad (6)$$

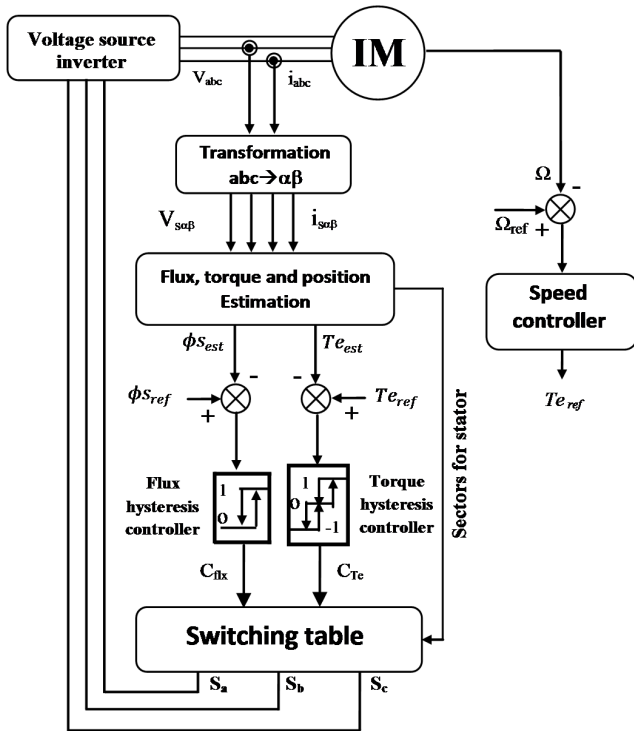


Fig. 1 Direct torque control (DTC) scheme for induction motor

The angle θ_s is given by (Eq. (7)):

$$\theta_s = \arctg \left(\frac{\varphi_{s\alpha}}{\varphi_{s\beta}} \right). \quad (7)$$

The error between the estimated and reference torques represents the input of a three level hysteresis comparator.

The purpose of the DTC for IM is to keep the stator flux and electromagnetic torque within the flux and torque hysteresis bands by correctly selecting the voltage vectors for the stator space during each sampling period (Fig. 2). The voltage vectors are selected according to the stator flux and torque errors [14, 15].

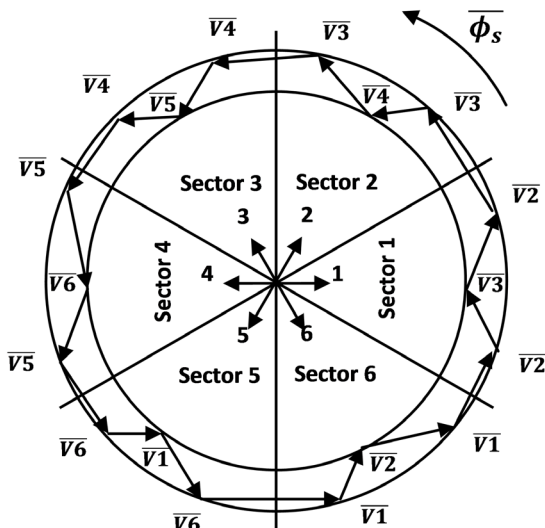


Fig. 2 Rotation of stator flux linkage vector by voltage vector

4 Controller's designs

4.1 PI anti-windup controller

Conventional PI controllers have an undesirable influence on the system response during a parametric variation [16]; moreover the setting of PI controllers does not generally take into account the physical limitations of the system such as the maximum current and voltage. For these reasons and in order to improve the dynamic responses of the machine in closed loop, we use a PI anti-windup controller [17] illustrated in Fig. 3. A PI anti-windup controller consists in taking into account the saturation a posteriori, to avoid or minimize the effect of the windup phenomenon in the integral actions of the PI, and to preserve the stability and the performances of the looped system, this controller makes it possible to improve the performances of the speed control by cancelling the saturation phenomenon caused by the saturation of the integrator [18].

4.2 First order sliding mode control (SMC)

Conventional PI controllers have two major drawbacks: sensitivity to variations in motor parameters and complexity of calculations. These control laws may be insufficient, especially when the requirements on accuracy, speed and other dynamic characteristics of the system are strict.

For this reason, it is necessary to use control laws that are insensitive to parameter variations, disturbances and non-linearity, such as the adaptive or absolute stability methods, but also the sliding mode technique. The latter is part of the theory of systems with variable structure [19, 20]. The expression of the control law is given by (Eq. (8)):

$$u = u_{eq} + u_n. \quad (8)$$

Considering the state system (Eq. (9)):

$$\dot{x} = A(x) + B(x)u. \quad (9)$$

In this study, we choose the error between the measured speed and the IM reference speed as the sliding mode surface S .

$\dot{S} = 0$ is a necessary condition for the state trajectory to remain on the switching surface and the equivalent control is obtained by recognising that $S = 0$ [21].

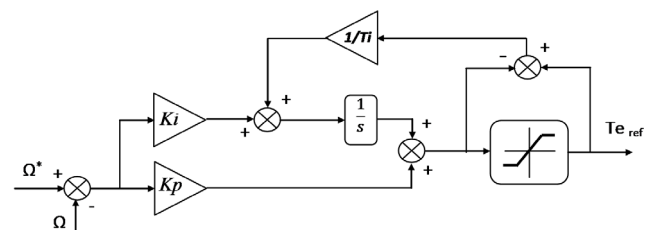


Fig. 3 PI anti-windup controller

The derivative of the sliding surface is given by (Eq. (10)):

$$\dot{S} = \frac{\partial S}{\partial r} = \frac{\partial S}{\partial x} \frac{\partial x}{\partial r}. \quad (10)$$

Replacing Eq. (9) and Eq. (10) with Eq. (8) gives the equivalent command u_{eq} :

$$\dot{S} = \frac{\partial S}{\partial x} A(x) + \frac{\partial S}{\partial x} B(x)u_{eq} + \frac{\partial S}{\partial x} B(x)u_n. \quad (11)$$

The equivalent control is defined during the slip phase and the steady state:

$$S = \dot{S} = 0 \text{ and } u_n = 0, \quad (12)$$

$$u_{eq} = -\left[\frac{\partial S}{\partial x} B(x)\right]^{-1} \frac{\partial S}{\partial x} A(x). \quad (13)$$

Equation (13) shows that the existence of an inverse matrix is necessary, which means the following condition:

$$\frac{\partial S}{\partial x} B(x) \neq 0. \quad (14)$$

By replacing Eq. (13) in Eq. (11), the new sliding surface expression becomes:

$$\dot{S} = \frac{\partial S}{\partial x} B(x)u_n. \quad (15)$$

The discontinuous control u_n is determined during the convergence state and must guarantee the finite time convergence condition $S \cdot \dot{S} < 0$ which is given by (Eq. (16)):

$$S \cdot \dot{S} = S \frac{\partial S}{\partial x} B(x)u_n < 0. \quad (16)$$

To satisfy this condition, the sign of one must be the opposite of the sign of $S \frac{\partial S}{\partial x} B(x)$.

The discontinuous control is defined as a switching term formed by the sign of the relay function (S) multiplied by a constant coefficient K , the relay function is defined by:

$$\text{sign}(S) = \begin{cases} +1 & \text{if } S \geq 0 \\ -1 & \text{if } S < 0 \end{cases} \quad (17)$$

The sliding surface of the rotor speed is defined by:

$$\begin{cases} S_\Omega = \Omega^* - \Omega \\ \dot{S} = \dot{\Omega}^* - \dot{\Omega} \end{cases} \quad (18)$$

So:

$$\dot{S}_\Omega = \dot{\Omega}^* - \frac{1}{J}(T_e - T_r - f_r \Omega). \quad (19)$$

According to the sliding mode theory we can write:

$$T_e = T_{eeq} + T_{en}, \quad (20)$$

with the equivalent control:

$$T_{eeq} = f_r \Omega + T_r, \quad (21)$$

and the discontinuous part:

$$T_{en} = k_\Omega \text{sign}(S_\Omega). \quad (22)$$

4.3 Second order sliding mode control (SOSMC)

The objective of this part is to generate a second-order sliding mode on a surface S by annulations of S and \dot{S} , ($S = \dot{S} = 0$), it signifies that the system converges to zero at the intersection of S and \dot{S} in the state space [21].

The reference torque generated by the second-order sliding mode controller is given by (Eq. (23)) [22]:

$$T_{e_ref} = T_{eeq} + u_{ST}. \quad (23)$$

The command law of the Super-Twisting algorithm is formed of two parts. The first V_1 is defined by its derivative with respect to time, while the second V_2 is continuous and according to the sliding variable (Eqs. (24) and (25)) [23, 24]:

$$u_{ST} = V_1(t) + V_2(t), \quad (24)$$

or:

$$\begin{cases} \dot{V}_1(t) = -A \text{sign}(S) + V_2(t) \\ V_2(t) = -B|S|^\delta \text{sign}(S) \end{cases} \quad (25)$$

Finally, the following conditions are given to ensure the convergence of slippery varieties:

$$\begin{aligned} A &> \frac{\lambda}{k_m} \\ B^2 &\geq \frac{4\lambda}{k_m^2 k_m (A - \lambda)} \\ 0 &< \delta < 0.5 \end{aligned} \quad (26)$$

4.4 Fuzzy-PI controller

In order to improve the performance of the DTC_IM we propose to use a fuzzy speed controller shown in Figs. 4 and 5.

The proposed controller is a hybrid controller with a fuzzy proportional-integral controller. The inputs of the fuzzy controller are the error and the error variation.

$$e = \Omega^* - \Omega \quad (27)$$

The proportional gain K_e makes fast corrections when a sudden change occurs at the input e . To eliminate the

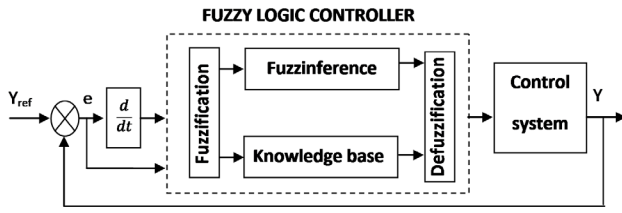


Fig. 4 General fuzzy controller structure

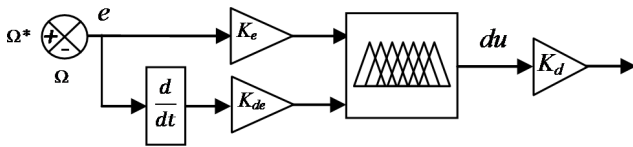


Fig. 5 Structure of fuzzy proportional-integral controller

stationary error, an integral action is required, which is why a PI is included in the controller [25, 26].

4.5 Hybrid fuzzy second order sliding mode control (FSOSMC)

In Section 4.5 we have thought of combining two already realized techniques (SOSMC and fuzzy controller) in order to obtain a hybrid controller that would combine the precision and speed of the fuzzy control with the simple and efficient structure of the second order sliding controller. This combination aims at keeping the robustness characteristics of the sliding controller while eliminating the undesirable effects probably caused by the existence of the sign function used in the SOSMC controller, replacing the sign function of the sliding controller by a fuzzy inference system [27]:

$$\dot{u}_1 = -\delta \text{fuzzy}(S_\Omega), \quad (28)$$

$$u_2 = -\lambda |S_\Omega|^\delta \text{fuzzy}(S_\Omega). \quad (29)$$

5 Particle swarm optimization

The selection of the appropriate values for the gains of each controller structure is often done by a hard trials-errors procedure. This tuning problem becomes difficult and delicate without a systematic design method.

In Section 5, the gains tuning problem, for all used controllers, is formulated as a constrained optimization problem which is solved by using the proposed PSO approach [28, 29]. The advantage of PSO over many other optimization algorithms is its relative simplicity and its characteristic of stable convergence with good computational efficiency.

At iteration k , a particle i in the swarm is characterized by [30]:

1. Position vector in a search space of D dimension:

$$\bar{x}_i^k = (x_{i1}^k, x_{i2}^k, \dots, x_{iD}^k). \quad (30)$$

2. Speed vector (velocity):

$$\bar{v}_i^k = (v_{i1}^k, v_{i2}^k, \dots, v_{iD}^k). \quad (31)$$

3. The position of the best solution through which it passed:

$$\bar{Pbest}_i^k = (pbest_{i1}^k, pbest_{i2}^k, \dots, pbest_{iD}^k). \quad (32)$$

4. The position of the best-known solution in its neighborhood: $gbest^k$.

5. The best position reached by the particles of the swarm is noted:

$$\bar{Gbest} = (gbest_1, gbest_2, \dots, gbest_D). \quad (33)$$

6. The fitness of its best solution: $fitpbest_i^k$.

7. The fitness of the best-known solution of its neighborhood: $fitgbest^k$.

At the start of the algorithm, the particles of the swarm are initialized at random/regular in the search space of the problem. At iteration $t + 1$, the velocity vector and position vector are calculated from Eq. (30) and Eq. (31), respectively [31, 32]:

$$v_i^{k+1} = \underbrace{\omega v_i^k}_{\text{Previous velocity}} + \underbrace{C_1 \text{rand}_1 (pbest_i^k - x_i^k)}_{\text{Cognitive component}} + \underbrace{C_2 \text{rand}_2 (gbest^k - x_i^k)}_{\text{Social component}}, \quad (34)$$

$$x_i^{k+1} = x_i^k + v_i^{k+1}, \quad (35)$$

where:

- $\omega, C_1, C_2 \geq 0$;
- ω : is the inertia weight factor;
- C_1 and C_2 : are the acceleration coefficients;
- rand_1 and rand_2 are two random numbers drawn uniformly in $[0, 1]$, at each iteration k .

Once the particles have been moved, the new positions are evaluated and the two vectors \bar{Pbest}_i and \bar{Gbest} are updated, at iteration $k + 1$, according to the two equations Eq. (32) and Eq. (33) respectively. This procedure is presented in Algorithm 1, where N is the number of particles in the swarm.

6 Simulation results and discussions

Simulation work has been performed to evaluate the performance of the proposed approaches applied to induction motor drives, the parameters are cited and presented in the Appendix. So, to illustrate the performance of the direct torque control of IM we replaced the classical PI speed

Algorithm 1 Particle swarm optimization algorithm (PSO)

1. Start
2. Randomly initialize N particles: position and velocity
3. Evaluate the positions of the particles
4. For each particle i , $\bar{P}_{best_i} = \bar{x}_i$
5. Calculate \bar{G}_{best} according to Eq. (33)
6. As long as the stopping criterion is not satisfied, do the following:
7. Move the particles according to Eq. (30) and Eq. (31)
8. Evaluate the positions of the particles
9. Update, \bar{P}_{best_i} and \bar{G}_{best} according to Eq. (32) and Eq. (33)
10. End

controller with five different controllers based on different techniques namely PI anti-windup, SMC, SOSMC, Fuzzy-PI and FSOSMC. A comparative study of the different controllers developed for the external speed loop of the DTC induction motor will be important to know which one gave better results. We consider two situations (see in Sections 6.1 and 6.2).

6.1 Situation 1: Step change in torque

Figs. 6 and 7 represents the waveforms of the improved speed and torque control performance.

The overall trends reflect the good dynamics of the control, a zoom on the speed drop due to the load clearly shows that the FSOSMC controller has better performances

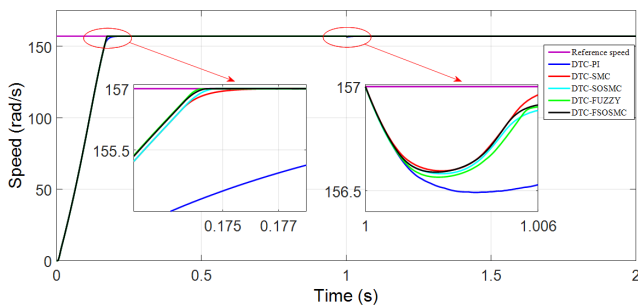


Fig. 6 Speed regulation obtained by the five control strategies. with applying load torque ($T_r = 25$ N m) at 1 second

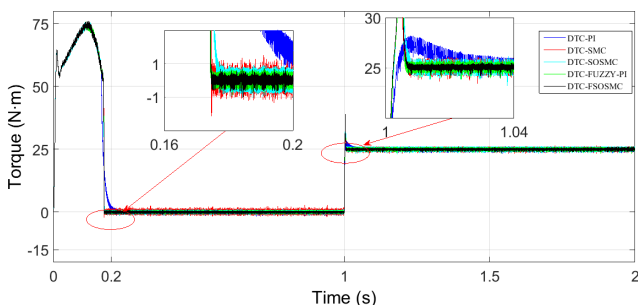


Fig. 7 Electromagnetic torque obtained by the five control strategies. with applying load torque ($T_r = 25$ N m) at 1 second

compared to the other controllers, the speed drop is minimal for the SMC, Fuzzy-PI and FSOSMC controllers but with faster rejection of the latter, with less torque ripple.

Table 1 gives an overview of the control dynamics with a comparative analysis of control systems with different speed controllers. It can be said that the Fuzzy-PI and FSOSMC controllers give the best dynamic performance with less torque ripple.

For the stator currents an FFT analysis of the stator current indicates a higher level of harmonics with the SMC controller, (Fig. 8(b)), the THD (total harmonic distortion) values show that the current with the FSOSMC controller is smoother compared to the other cases while the fuzzy controller has the closest THD which means the efficiency of this controller. These results confirm the study carried out in references [33–35].

The main reason for the torque (current) ripple in the conventional DTC is that the selected voltage vector applies for the complete switching period, regardless of the magnitude of the torque error, resulting in a wide torque hysteresis band. A better drive performance can be achieved by varying the duration of applying the selected voltage vector during each switching period, according to the magnitude of the torque error and the position of the stator flux, which will result in a small torque hysteresis band and hence less torque ripple (current) and therefore a reduction of the THD of the stator current.

Table 2 approves the previous results using the most used performance indices in articles, academic journals and simulation studies:

- Integral Squared Error (ISE): $ISE = \int e^2 dt$;
- Integral Absolute Error (IAE): $IAE = \int |e| dt$;
- Integral Time – weighted Absolute Error (ITAE): $ITAE = \int t|e| dt$.

6.2 Situation 2: Stator resistance variations

In the DTC, the stator flux linkage was estimated by Eq. (5). But some problems occur when the IM is operated at very low speeds. Indeed, if the motor stator resistance will be different from that used in flux estimator, the inverter may be unstable at low speeds with a high load.

The stator resistance can vary from about 1.5 to 1.7 times its nominal value. The control system becomes unstable if the value of this resistance used in the control is different from that of the machine.

Two possible cases:

1. The actual resistance is higher than the one used in the control due to the increase in temperature of the machine.

Table 1 Comparative study between five control strategies

	Speed setting time (seconds)	Speed drop due to the load torque (rad/s)	Ripple flux (value max – value min) (Wb)	Torque ripple (value max – value min) (N m)	THD (%)
DTC_PI anti-windup	0.1570	156.7	0.0135	1.60	2.24
DTC_SMC	0.1770	156.6	0.0127	1.63	2.28
DTC_SOSMC	0.1747	156.6	0.0120	1.61	2.02
DTC_Fuzzy	0.1743	156.6	0.0114	1.05	1.92
DTC_FSOSMC	0.1744	156.6	0.0103	0.54	1.66

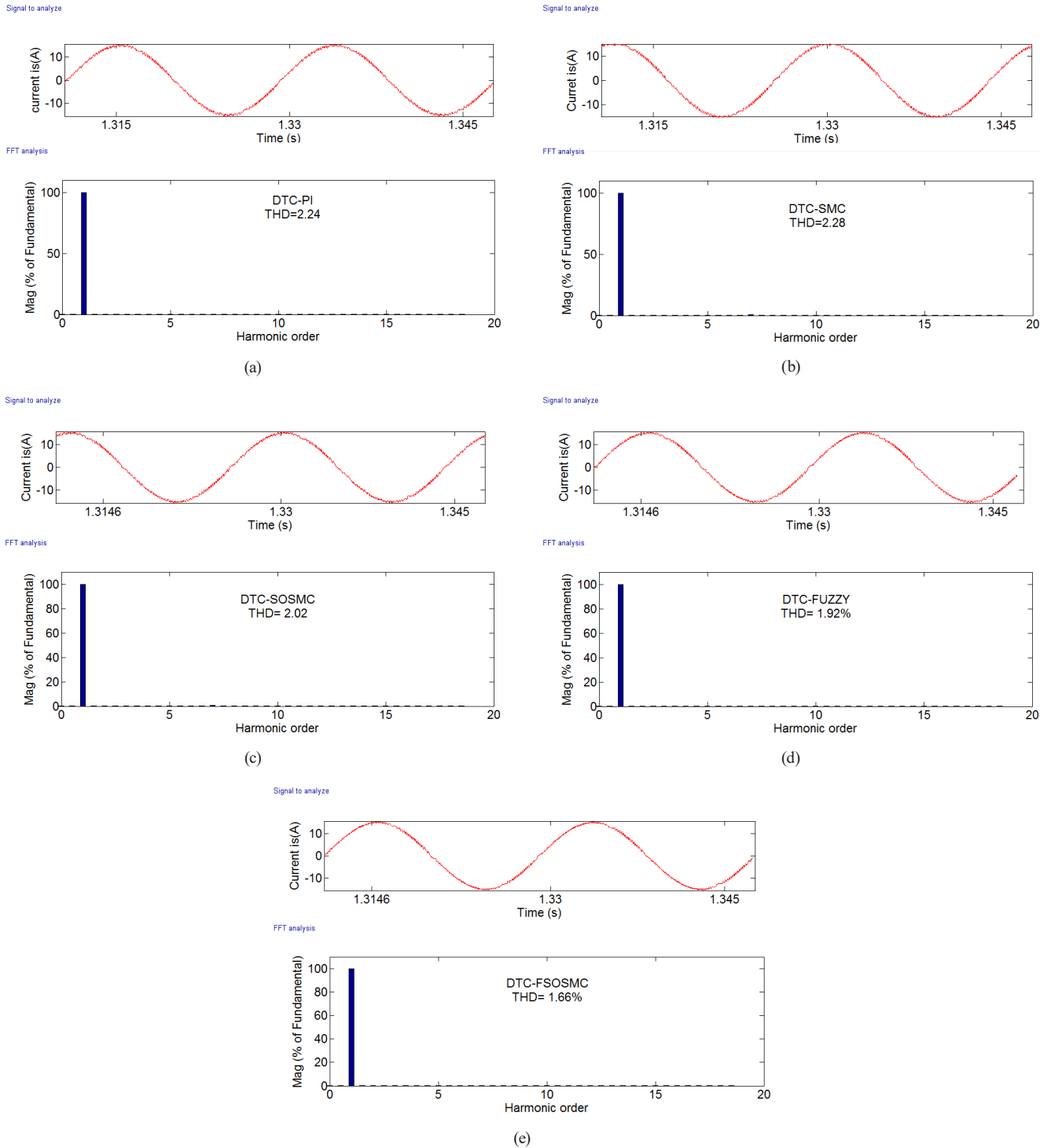


Fig. 8 Steady-state stator phase currents and harmonic spectrum at 157 rad/s and 25 N m; (a) DTC-PI Anti-Windup; (b) DTC-SMC; (c) DTC-SOSMC; (d) DTC-FUZZY; (e) DTC-FSOSMC

Table 2 Comparison of performance index

	IAE	ISE	ITAE
DTC_PI anti-windup	14.4	1587	0.8444
DTC_SMC	14.38	1589	0.8341
DTC_SOSMC	14.42	1589	0.8307
DTC_Fuzzy	14.44	1587	0.972
DTC_FSOSMC	14.42	1587	0.9357

2. The resistance may be lower than the rated value in a drive system in colder climates.

To study the performance of the different approaches and the influence of the stator resistance change, simulation tests were performed. The stator resistance value was changed from 1.2Ω to 1.8Ω from 1 to 1.5 seconds, followed by a 50% decrease from its nominal value at 1.5 seconds. The reference torque and reference flux were kept constant at 25 N m and 1 Wb, with a low reference speed of 25 rad/s. Figs. 9, 10, 11, 12 and 13 shows the simulation results for stator resistance change, where the flux estimator has the nominal value of stator resistance but the actual stator resistance increased by 50% of its nominal value then decrease by 50%.

For a PI controller the results show the influence of the stator resistance on the behavior of the machine for low speeds where the stator flux loses stability with the change

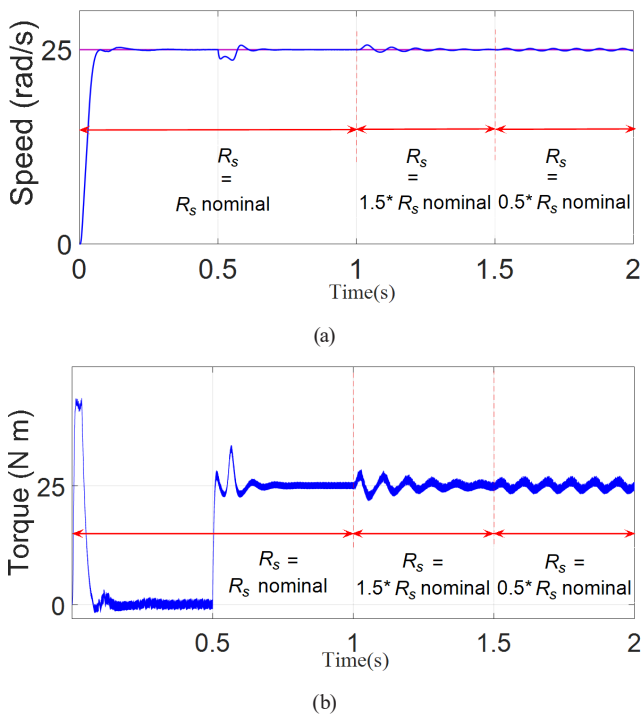


Fig. 9 DTC-PI Anti-Windup compartment with rotor resistance variation (torque load $T_r = 25$ N m at $t = 0.5$ s, $R_s = 1.5 R_s$ nominal at $t = 1$ s and $R_s = 0.5 R_s$ nominal at $t = 1.5$ s); (a) Speed; (b) Torque

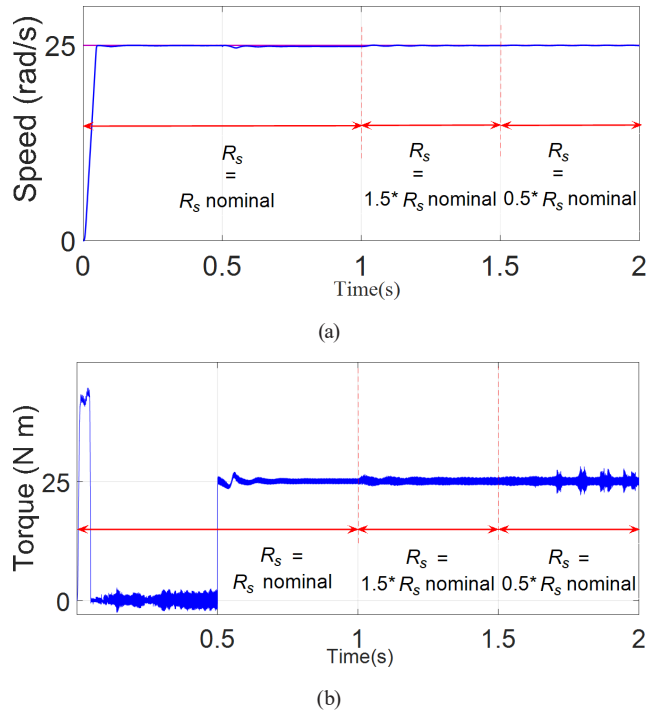


Fig. 10 DTC-SMC compartment with rotor resistance variation (torque load $T_r = 25$ N m at $t = 0.5$ s, $R_s = 1.5 R_s$ nominal at $t = 1$ s and $R_s = 0.5 R_s$ nominal at $t = 1.5$ s); (a) Speed. (b) Torque

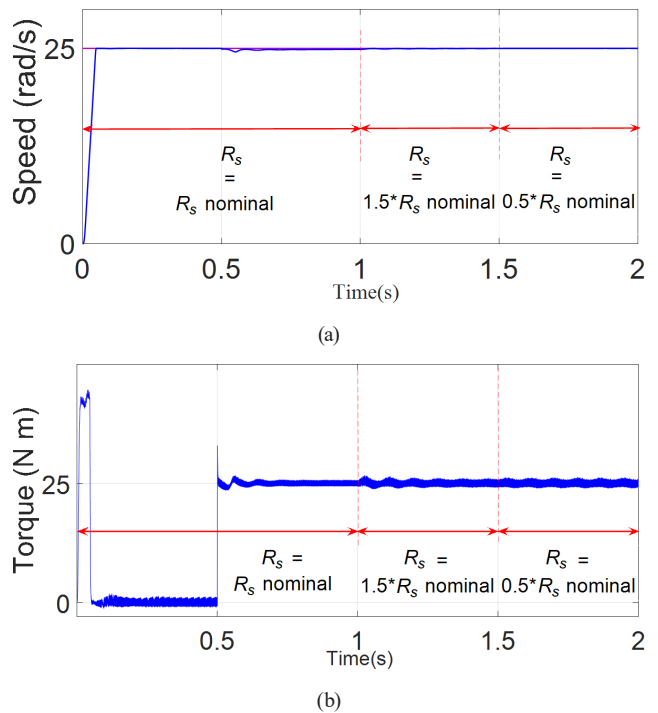


Fig. 11 DTC-SOSMC compartment with rotor resistance variation (torque load $T_r = 25$ N m at $t = 0.5$ s, $R_s = 1.5 R_s$ nominal at $t = 1$ s and $R_s = 0.5 R_s$ nominal at $t = 1.5$ s); (a) Speed; (b) Torque

of the resistance value this disturbance also influences the mechanical responses i.e. speed and torque, on the other side the system response for the other controllers is very

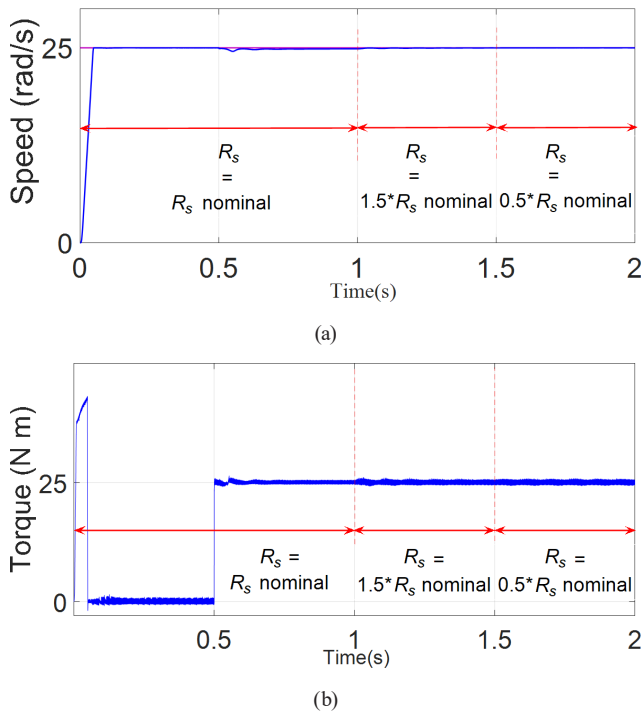


Fig. 12 DTC-Fuzzy comportment with rotor resistance variation (torque load $T_r = 25$ N m at $t = 0.5$ s, $R_s = 1.5 R_s$ nominal at $t = 1$ s and $R_s = 0.5 R_s$ nominal at $t = 1.5$ s); (a) Speed; (b) Torque

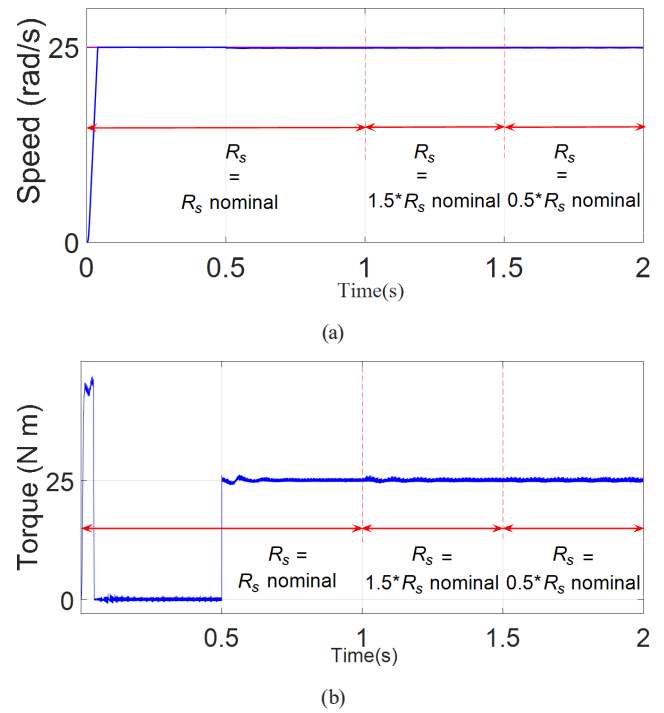


Fig. 13 DTC-FSOSMC comportment with rotor resistance variation (torque load $T_r = 25$ N m at $t = 0.5$ s, $R_s = 1.5 R_s$ nominal at $t = 1$ s and $R_s = 0.5 R_s$ nominal at $t = 1.5$ s); (a) Speed; (b) Torque

satisfactory where the mechanical response of the machine is very smooth with greater stability without any undesirable influence. We find that the use of these controllers leads to a clear improvement of the dynamic response, with a remarkable superiority of FSOSMC, this controller has overcome the problem of low speed operation, in addition to the significant reduction of torque ripples.

7 Conclusion

In this paper, five modern structures of speed controllers optimized by a PSO algorithm associated with a DTC control of an induction machine has been discussed and analyzed. The objective is to improve the performance of the DTC, the aim of this improvement is to minimize the torque and flux ripples of the IM on the one hand and to ensure a smooth and fast speed response of the controller and a robust response against parameter variation and satisfactory even at low speed on the other hand. A comparative analysis is performed between PI anti-windup, first and second sliding mode, fuzzy and hybrid fuzzy second

order sliding controller under different operating conditions. The simulation results obtained show the contribution of each controller in improving the performance of the DTC, it is evident that the hybrid FSOSMC controller has better performance than other controllers with a significant reduction in torque, flux and stator current ripples (THD = 1.66%) and improved robustness against parameter variation (stator resistance) and external perturbations (load torque) which is confirmed by the results of Table 1. Torque accuracy and speed control are maintained at low speeds. Using an FSOSMC speed controller with DTC in areas exposed to severe weather conditions such as extreme heat or cold is a good solution for direct torque control efficiency as it is not affected by any parameter change of the machine. It can also be used in applications requiring precise and fast response.

It can be concluded that the techniques proposed in this work contribute to the realization of these goals and performances, as well as great prospects for optimizing the DTC drive.

References

- [1] De Klerk, M. L., Saha, A. K. "A Comprehensive Review of Advanced Traction Motor Control Techniques Suitable for Electric Vehicle Applications", *IEEE Access*, 9, pp. 125080–125108, 2021. <https://doi.org/10.1109/ACCESS.2021.3110736>
- [2] Boubzizi, S., Abid, H., El hajjaji, A., Chaabane, M. "Comparative study of three types of controllers for DFIG in wind energy conversion system", *Protection and Control of Modern Power Systems*, 3(1), 21, 2018. <https://doi.org/10.1186/s41601-018-0096-y>
- [3] Oliveira, C. M. R., Aguiar, M. L., Monteiro, J. B. A., Pereira, W. C., Paula, G. T., Santana, M. P. "Vector Control of Induction Motor using a Sliding Mode Controller with Chattering Reduction", In: 2015 IEEE 13th Brazilian Power Electronics Conference and 1st Southern Power Electronics Conference (COBEP/SPEC), Fortaleza, Brazil, 2015, pp. 1–6. ISBN 978-1-4799-8779-5 <https://doi.org/10.1109/COBEP.2015.7420071>
- [4] Eldigair, Y., Garelli, F., Kunusch, C., Ocampo-Martinez, C. "Adaptive PI control with robust variable structure anti-windup strategy for systems with rate-limited actuators: Application to compression systems", *Control Engineering Practice*, 96, 104282, 2020. <https://doi.org/10.1016/j.conengprac.2019.104282>
- [5] Fdaili, M., Essadki, A., Nasser, T. "Comparative Analysis Between Robust SMC & Conventional PI Controllers Used in WECS Based on DFIG", *International Journal of Renewable Energy Research-IJRER*, 7(4), pp. 2151–2161, 2017. <https://doi.org/10.20508/ijrer.v7i4.6441.g7267>
- [6] Elsherbiny, H., Ahmed, M. K., Elwany, M. "Comparative Evaluation for Torque Control Strategies of Interior Permanent Magnet Synchronous Motor for Electric Vehicles", *Periodica Polytechnica Electrical Engineering and Computer Science*, 65(3), pp. 244–261, 2021. <https://doi.org/10.3311/PPee.16672>
- [7] Yaichi, I., Semmah, A., Wira, P., Djeriri, Y. "Super-twisting Sliding Mode Control of a Doubly-fed Induction Generator Based on the SVM Strategy", *Periodica Polytechnica Electrical Engineering and Computer Science*, 63(3), pp. 178–190, 2019. <https://doi.org/10.3311/PPee.13726>
- [8] Sellah, M., Abdellah, K., Rezaoui, M. M. "Investigation of SVPWM Based Sliding Mode Control Application on Dual-Star Induction Motor and Dual Open-End Winding Induction Motor", *Periodica Polytechnica Electrical Engineering and Computer Science*, 66(1), pp. 80–98, 2022. <https://doi.org/10.3311/PPee.17910>
- [9] Li, H., Maghareh, A., Wilfredo Condori Uribe, J., Montoya, H., Dyke, S., Xu, Z. "An adaptive sliding mode control system and its application to real-time hybrid simulation", *Structural Control Health Monitoring*, 29(1), e2851, 2022. <https://doi.org/10.1002/stc.2851>
- [10] Laggoun, L., Kiyyour, B., Boukhalfa, G., Belkacem, S., Benagoune, S. "Direct Torque Control Using Fuzzy Second Order Sliding Mode Speed Regulator of Double Star Permanent Magnet Synchronous Machine", In: *Proceedings of the 4th International Conference on Electrical Engineering and Control Applications, ICEECA 2019, Constantine, Algeria, 2019*, pp. 139–153. ISBN 978-981-15-6402-4 https://doi.org/10.1007/978-981-15-6403-1_10
- [11] Chakir El Alaoui, E., Ayad, H., Doubabi, S. "Fuzzy Anti-Windup Schemes for PID Controllers", *International Journal of Applied Engineering Research*, 1(3), pp. 295–306, 2006. [online] Available at: https://www.researchgate.net/publication/228647370_Fuzzy_Anti-Windup_Schemes_for_PID_Controllers [Accessed: 05 February 2023]
- [12] Sartorius-Castellanos, A. R., Moreno-Vázquez, J. de J., Antonio-Ortiz, R., Hernández-Nieto, M. L. "A novel method for fuzzy scale factors scheduling in fuzzy PD+I with anti-windup system controllers", *Revista Facultad De Ingeniería Universidad De Antioquia*, 80, pp. 142–151, 2016. <https://doi.org/10.17533/udea.redin.n80a15>
- [13] Takahashi, I., Noguchi, T. "A New Quick-Response and High-Efficiency Control Strategy of an Induction Motor", *IEEE Transactions on Industry Applications*, IA-22(5), pp. 820–827, 1986. <https://doi.org/10.1109/TIA.1986.4504799>
- [14] Aktas, M., Awaili, K., Ehsani, M., Arisoy, A. "Direct torque control versus indirect field-oriented control of induction motors for electric vehicle applications", *Engineering Science and Technology, an International Journal*, 23(5), pp. 1134–1143, 2020. <https://doi.org/10.1016/j.jestech.2020.04.002>
- [15] Vas P. "Sensorless Vector and Direct Torque Control", Oxford University Press, 1998. ISBN 9780198564652
- [16] Dekali, Z., Baghli, L., Boumediene, A. "Improved Super Twisting Based High Order Direct Power Sliding Mode Control of a Connected DFIG Variable Speed Wind Turbine", *Periodica Polytechnica Electrical Engineering and Computer Science*, 65(4), pp. 352–372, 2021. <https://doi.org/10.3311/PPee.17989>
- [17] Talib, M. H. N., Ibrahim, Z., Rahim, N. A., Hasim, A. S. A. "Comparison Analysis of Indirect FOC Induction Motor Drive using PI, Anti-Windup and Pre Filter Schemes", *International Journal of Power Electronics and Drive Systems (IJPEDS)*, 5(2), pp. 219–229, 2014. <https://doi.org/10.11591/ijpeds.v4i4.6250>
- [18] Aichi, B., Kendouci, K. "A Novel Switching Control for Induction Motors Using a Robust Hybrid Controller that Combines Sliding Mode with PI Anti-Windup", *Periodica Polytechnica Electrical Engineering and Computer Science*, 64(4), pp. 392–405, 2020. <https://doi.org/10.3311/PPee.15661>
- [19] El Daoudi, S., Lazrak, L., Ait Lafkih, M. "Sliding mode approach applied to sensorless direct torque control of cage asynchronous motor via multi-level inverter", *Protection and Control of Modern Power Systems*, 5(1), 13, 2020. <https://doi.org/10.1186/s41601-020-00159-7>
- [20] Kelkoul, B., Boumediene, A. "Stability analysis and study between classical sliding mode control (SMC) and super twisting algorithm (STA) for doubly fed induction generator (DFIG) under wind turbine", *Energy*, 214, 118871, 2021. <https://doi.org/10.1016/j.energy.2020.118871>
- [21] Bartolini, G., Ferrara, A., Levant, A., Usai, E. "On Second Order Sliding Mode Controllers", In: Young, K. D., Özgüner, Ü. (eds.) *Variable Structure Systems, Sliding Mode and Nonlinear Control*, Springer-Verlag, 1999, pp. 329–350. ISBN 978-1-85233-197-9 <https://doi.org/10.1007/BFb0109984>

- [22] Ammar, A., Bourek, A., Benakcha, A. "Sensorless SVM-direct torque control for induction motor drive using sliding mode observers", *Journal of Control, Automation and Electrical Systems*, 28(2), pp. 189–202, 2017.
<https://doi.org/10.1007/s40313-016-0294-7>
- [23] Lin, W.-B., Chiang, H.-K. "Super-Twisting Algorithm Second-Order Sliding Mode Control for a Synchronous Reluctance Motor Speed Drive", *Mathematical Problems in Engineering*, 2013, 632061, 2013.
<https://doi.org/10.1155/2013/632061>
- [24] Bartolini, G., Pisano, A., Usai, E. "Second-order sliding-mode control of container cranes", *Automatica*, 38(10), pp. 1783–1790, 2002.
[https://doi.org/10.1016/S0005-1098\(02\)00081-X](https://doi.org/10.1016/S0005-1098(02)00081-X)
- [25] Ding, X., Liu, Q., Ma, X., He, X., Hu, Q. "The Fuzzy Direct Torque Control of Induction Motor Based on Space Vector Modulation", In: *Third International Conference on Natural Computation (ICNC 2007)*, Haikou, China, 2007, pp. 260–264. ISBN 978-0-7695-2875-5
<https://doi.org/10.1109/ICNC.2007.726>
- [26] Saidi, A., Nacéri, F., Youb, L., Cernat, M., Guasch Pesquer, L. "Two Types of Fuzzy Logic Controllers for the Speed Control of the Doubly-Fed Induction Machine", *Advances in Electrical and Computer Engineering*, 20(3), pp. 65–74, 2020.
<https://doi.org/10.4316/AECE.2020.03008>
- [27] Cherifi, D., Miloud, Y. "Hybrid Control Using Adaptive Fuzzy Sliding Mode Control of Doubly Fed Induction Generator for Wind Energy Conversion System", *Periodica Polytechnica Electrical Engineering and Computer Science*, 64(4), pp. 374–381, 2020.
<https://doi.org/10.3311/PPee.15508>
- [28] Wang, D., Tan, D., Liu, L. "Particle swarm optimization algorithm: an overview", *Soft Computing*, 22(2), pp. 387–408, 2018.
<https://doi.org/10.1007/s00500-016-2474-6>
- [29] Vijay, M., Jena, D. "PSO based neuro fuzzy sliding mode control for a robot manipulator", *Journal of Electrical Systems and Information Technology*, 4(1), pp. 243–256, 2017.
<https://doi.org/10.1016/j.jesit.2016.08.006>
- [30] Boukhalifa, G., Belkacem, S., Chikhi, A., Benaggoune, S. "Direct torque control of dual star induction motor using a fuzzy-PSO hybrid approach", *Applied Computing and Informatics*, 18(1/2), pp. 74–89, 2022.
<https://doi.org/10.1016/j.aci.2018.09.001>
- [31] Bouchakour, A., Borni, A., Brahami, M. "Comparative study of P&O-PI and fuzzy-PI MPPT controllers and their optimisation using GA and PSO for photovoltaic water pumping systems", *International Journal of Ambient Energy*, 42(15), pp 1746–1757, 2021.
<https://doi.org/10.1080/01430750.2019.1614988>
- [32] Wang, H., Fei, Y., Li, Y., Ren, S., Che, J., Xu, H. "Particle Swarm Optimization with Power-Law Parameter Based on the Cross-Border Reset Mechanism", *Advances in Electrical and Computer Engineering*, 17(4), pp. 59–68, 2017.
<https://doi.org/10.4316/AECE.2017.04008>
- [33] Mazouz, F., Belkacem, S., Colak, I. "DPC- SVM of DFIG Using Fuzzy Second Order Sliding Mode Approach", *International Journal of Smart Grid – ijSmartGrid*, 5(4), pp. 174–182, 2021.
<https://doi.org/10.20508/ijsmartgrid.v5i4.219.g178>
- [34] Zaihidee, F. M., Mekhilef, S., Mubin, M. "Robust Speed Control of PMSM Using Sliding Mode Control (SMC)—A Review", *Energies*, 12(9), 1669, 2019.
<https://doi.org/10.3390/en12091669>
- [35] Ahammad, T., Beig, A. R., Al-Hosani, K. "Sliding mode based DTC of three-level inverter fed induction motor using switching vector table", In: *2013 9th Asian Control Conference (ASCC)*, Istanbul, Turkey, 2013, pp. 1–6. ISBN 978-1-4673-5767-8
<https://doi.org/10.1109/ASCC.2013.6606261>

Appendix

Table A1 Parameters of the induction motor

Stator resistance	$R_s = 1.2 \Omega$
Rotor resistance	$R_r = 1.8 \Omega$
Stator inductance	$L_s = 0.1554 \text{ H}$
Rotor inductance	$L_r = 0.1568 \text{ H}$
Mutual inductance	$L_m = 0.15 \text{ H}$
Viscous friction coefficient	$f_r = 0.001 \text{ N m s rad}^{-1}$
Machine inertia	$J = 0.0662 \text{ kg m}^2$